PHYSICAL REVIEW B **78**, 174409 (2008)

Magnetic ordering in the double-layered molecular magnet Cu(tetren)[W(CN)$_8$]: Single-crystal study

Maria Bałanda, Robert Pełka,* and Tadeusz Wasiutyński
H. Niewodniczański Institute of Nuclear Physics, Polish Academy of Sciences, Radzikowskiego 152, 31-342 Kraków, Poland

Michał Rams
Institute of Physics, Jagiellonian University, Reymonta 4, 30-059 Kraków, Poland

Yasuhiro Nakazawa, Yuji Miyazaki, and Michio Sorai
Research Center for Molecular Thermodynamics, Graduate School of Science, Osaka University, Toyonaka, Osaka 560-0043, Japan

Robert Podgajny, Tomasz Korzeniak, and Barbara Sieklucka
Department of Chemistry, Jagiellonian University, Ingardena 3, 30-060 Kraków, Poland

(Received 3 September 2008; revised manuscript received 10 October 2008; published 10 November 2008)

The results of the single-crystal studies of the quasi-two-dimensional (2D) copper-octacyanotungstenate coordination polymer $\{(\text{tetrenH}_5)_{0.8}\text{Cu}^{\text{II}}_4[\text{W}^{\text{V}}(\text{CN})_8]_4\cdot 7.2\text{H}_2\text{O}\}_n$ are presented. It was found that the three-dimensional (3D) magnetic ordering at $T_c \approx 33$ K gives rise to antiferromagnetic structure which under relatively small magnetic field changes to ferromagnetic. There is strong easy-plane anisotropy confining the magnetic moments to the *ac* crystallographic plane. Detailed analysis of the scaling behavior of the dc susceptibility above T_c is performed. For the direction of the external magnetic field parallel to the *ac* crystallographic plane the ordering process involves one stage only, whereas for the direction parallel to the *b* crystallographic axis a two-stage process is revealed. The corresponding crossover at about 39 K is from the 2D short-range order state to the 3D long-range one. The well-established short-range order above the transition is consistent with the low value of the entropy amounting to only 15% of the maximal expected value. The scaling behavior of the Berezinski-Kosterlitz-Thouless type has been checked for the temperature dependence of magnetization in the *ac* plane yielding the value of $\nu=0.56$. The spin-flip field is explained by assuming that below the transition temperature there is a domain structure coupled through the dipole-dipole interactions. The ratio of the interbilayer to the intrabilayer exchange interaction was estimated to amount to 1×10^{-4}.

DOI: 10.1103/PhysRevB.78.174409 PACS number(s): 75.25.+z, 75.30.Cr, 75.40.Cx, 75.40.Gb

I. INTRODUCTION

Magnetic materials of reduced dimensionality have been of much interest for more than two decades. The last years marked by a growing interest in synthesizing new molecular magnets still open up additional perspectives.[1,2] The advanced modern chemistry enables one to obtain a wide scope of metal-organic systems: besides three-dimensional (3D) magnets,[3] one can study two-dimensional (2D) systems,[4] one-dimensional (1D) molecular chains,[5] or high-spin molecules (0D).[6] While the last two types, representing molecule-based nanomagnets, are currently in the focus of research due to their specific relaxation properties, the two-dimensional molecular networks are attractive due to their peculiar phase diagram in the applied field and as an alternative source of technologically important magnetic multilayers.[7] The molecular magnetic materials are often built of one-dimensional or two-dimensional spin clusters where coupling J between magnetic moments within the cluster is ensured by appropriate molecular bridges and the correlation length grows on cooling the system. Dipolar interactions J' of the clusters resultant magnetic moments may trigger transition to the long-range ordered state and stabilize the spontaneous magnetization. An interesting problem discussed for the 2D lattices is the role of the intralayer anisotropy (Ising, *XY*, or anisotropic Heisenberg type) and of the interlayer coupling J' in the occurrence and type of the phase transition. It is known[8] that for a 2D Heisenberg magnet the transition to the ordered state can occur only at $T_c=0$, but for the 2D *XY* model the topological phase transition caused by the unbinding of vortex-antivortex pairs may take place at a critical temperature T_{BKT}, where BKT stands for Berezinski-Kosterlitz-Thouless, as predicted by Berezinskii,[9] Kosterlitz and Thouless.[10,11] While for the infinite system magnetization at $T<T_{\text{BKT}}$ is zero, the finite-size 2D *XY* sample will have magnetic moment. It was shown by Bramwell and Holdsworth[12] that the universal signature of a finite-sized 2D *XY* behavior is a critical exponent $\beta=0.23$. Such value had been already observed for an array of layered magnets with nonzero interplane coupling and thin films.[13,14]

The present work is devoted to the unusual properties of a 2D molecular magnet belonging to compounds built on octacyanometallate $[M(\text{CN})_8]^{3-}$ ($M=\text{Mo}^{\text{V}},\text{W}^{\text{V}}$) and a 3D cationic paramagnetic complex. Octacyanometallates are good and versatile building blocks for constructing molecular magnetic materials because they adopt to various structures depending on the surrounding ligands, and besides, the cyanide groups efficiently connect spin densities at metal centers.[15] The subject of the study is the copper-tungsten cyanide coordination polymer $\{(\text{tetrenH}_5)_{0.8}\text{Cu}^{\text{II}}_4[\text{W}^{\text{V}}(\text{CN})_8]_4\cdot 7.2\text{H}_2\text{O}\}_n$ (tetren =tetraethylenepentaamine) hereafter abbreviated as WCuT

 ©2008 The American Physical Society

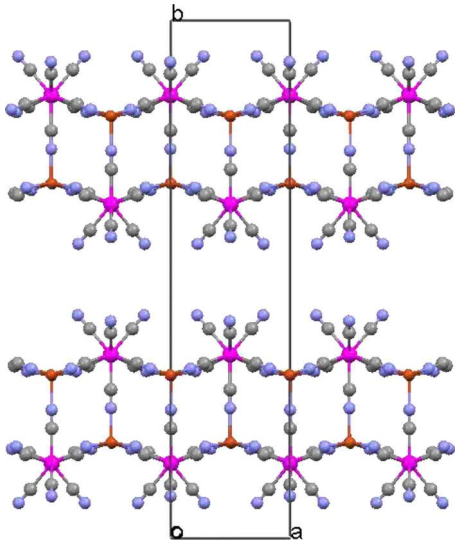

FIG. 1. (Color online) Crystal structure of $Cu_4[W(CN)_8]_4$ seen along the crystallographic axis *c*: W – dark gray, Cu – light gray, C – gray.

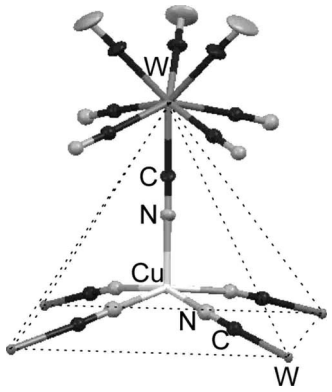

FIG. 2. The square-pyramidal building unit of the double-layer sheets. Each copper center is surrounded by five cyanide bridges linking it to the neighboring tungsten centers. The coordination sphere of the tungsten center comprises eight cyanide ligands, five of which link it to the neighboring copper centers. The three remaining ones stand out of the *ac* plane and are presumably involved in the network of hydrogen bonds linking the bilayers through the lattice water molecules. The apical cyanide bridge is almost linear, whereas the equatorial ones are slightly bent.

which was first reported by Podgajny *et al.*[16] In Refs. 16–19 measurements carried out on powder samples by means of different techniques, i.e., ac and dc magnetometries, adiabatic calorimetry, and μSR were reported. An anomalous behavior of ac susceptibility at the transition point $T_c=33.4$ K was noticed as well as the metamagnetic features below T_c. In particular, the critical exponent of the magnetic order parameter obtained from μSR (Ref. 19) pointed to the 2D magnetic topology of our system and was close to the value predicted for the BKT transition.

WCuT crystallizes in orthorhombic crystallographic system (space-group $Cmc2_1$) with unit-cell parameters $a=7.3792(6)$ Å, $b=32.096(2)$ Å, and $c=7.0160(6)$ Å. It is built of cyanobridged copper-tungsten anionic double-layer sheets lying in the *ac* plane. The space between the double layers is filled with water molecules and tetrenH_5^{5+} solvent molecules. The spin carriers in the system are Cu^{II} ($S=1/2$) and W^V ($S=1/2$) ions. The structure projected onto the *ab* plane is shown in Fig. 1. Figure 2 shows the square-pyramidal building unit of the double-layer sheets. The thickness of the double layers, measured as the length of the axial Cu-N-C-W linkage, is equal to 5.37 Å. The distance between the double layers is about 10 Å as the interatomic W-W and W-Cu distances between the double layers are 9.96 and 11.22 Å, respectively. The unit cell contains four $Cu^{II}W^V$ units.

Magnetic measurements carried out for a powder sample revealed an unconventional behavior of this system. Dc susceptibility measured in the paramagnetic region showed ferromagnetic correlations with a positive Curie-Weiss temperature $\theta\approx(44\pm2)$ K and Curie constant equal to (4.2 ± 0.3) emu K/mol. The appearance of the magnetically ordered state at $T_c=33.4$ K is manifested by the sharp ac susceptibility peak and a heat-capacity anomaly with the entropy gain $\Delta S=R$ ln 2 that is only 13% of the maximal value expected for eight one-half spins. The exceptionally narrow χ_{ac} peak at T_c (0.8 K at half-height) and an almost zero value recorded[18] for WCuT sample at $T<T_c$ resembled the magnetic response of ferromagnetic thin films.[20,21] In the latter case, the ac driving field is too weak, as compared to the anisotropy field, to reconstruct the domains. Both the amplitude H_{ac} of the oscillating field and that of the dc external field caused significant changes in χ_{ac}, which were more pronounced in the temperature range below T_c than in the peak itself. Like for metamagnets, the typically ferromagnetic χ_{ac} response appeared only for H_{dc} stronger than the threshold value. The field-induced ferromagnetic behavior was combined with weak glasslike properties, as documented by checking the dependence of the χ' peak temperature T_p on the frequency of the oscillating field. A hysteresis loop at $T=4.3$ K with weak coercive field H_c of 80 Oe and the remnant magnetization M_R of $1.04\mu_B$ was typical of a rather soft ferromagnet. The magnetization of $7.8\mu_B$ at high field (56 kOe) was close to the expected $8\mu_B$ for ferromagnetically coupled Cu^{II}-W^V ions. Based on the results above, the WCuT was understood as a set of ferromagnetic double layers interacting with neighboring bilayers with weak antiferromagnetic forces.

The muon spin rotation and relaxation experiment performed by Pratt *et al.*[19] still supplied more information on the magnetic ordering and nature of the field-induced metamagnetic transformation. A μSR precession signal in the magnetically ordered state contained two components of the local magnetic field B_1 and B_2. The temperature dependence of both components was fitted to the phenomenological function $B_i(T)=B_i(0)[1-(T/T_c)^\alpha]^\beta$. The parameter α refers to the low T properties governed by spin-wave excitations, whereas β determines the asymptotic critical behavior close to the transition. The parameters were determined simultaneously from fitting both sets of local fields over the full temperature range 5–33 K giving $\beta=0.237(12)$ and $\alpha=1.84(15)$. The critical exponent β is close to that predicted for a 2D *XY* system where a Berezinski-Kosterlitz-Thouless transition

takes place. Independently, the field-induced metamagnetic spin reorientation process was directly monitored with the μSR technique.

The present work devoted to the investigation of the single-crystal sample brings experimental results on metamagnetism, magnetization behavior at T_c, and magnetic anisotropy below and above the transition. The critical scaling analysis of the susceptibility in the temperature region above the transition is reported. Additionally magnetic anisotropy is analyzed based on the dipolar interaction. The system under study is an example of a real magnet based on the $S=1/2$ spins in which the 2D character is clearly demonstrated above as well as below the phase transition.

II. EXPERIMENTAL DETAILS

Single crystals of WCuT of dimensions of an order of millimeter were grown. The transparent light green crystals grow in the form of petals $\approx$0.1 mm thin. The face of petal corresponds to *ac* crystallographic plane. The detailed method of the synthesis was described earlier.[16] dc magnetization data were obtained with a Quantum Design magnetometer, model MPMS 5XL. The data were corrected for the diamagnetic and temperature independent paramagnetism contributions. On the basis of the sample dimensions ($2.1\times2.7\times0.08$ mm^3) the demagnetization factors were estimated; $N_{\parallel}=4\pi\times0.03$ and $N_{\perp}=4\pi\times0.94$. Due to the demagnetization correction the changes in the best-fit parameters for the field parallel to the *ac* crystallographic plane amounted to 0.02%. For the field parallel to the *b* crystal axis the corresponding changes were of the order of 3%. In both cases the parameter changes were below the statistical errors. In the zero-field-cooling (ZFC) regime, the sample was cooled in zero magnetic field then the field was switched on, and magnetization was measured on heating in this field. In the field-cooling (FC) regime, the sample was cooled in field and subsequently measured in this field on heating. The heat-capacity measurements in the external magnetic field up to 9 T were carried out using Quantum Design physical property measurement system in the Research Center for Molecular Thermodynamics at Osaka University. To ensure a good thermal contact, the single-crystal petal was attached to the measuring unit so that the *b* crystallographic axis coincided with the direction of the external field.

III. EXPERIMENTAL RESULTS

A. dc magnetization

The dc measurements of the single-crystal sample of mass $\approx$1 mg were performed for two different orientations with respect to the applied field, i.e., with the field parallel and perpendicular to the *ac* crystallographic plane.

Figure 3(a) shows the result of the measured magnetization on cooling in the external field of 2 kOe. The magnetic ordering manifests itself in different ways in the two directions. The magnetization measured in the *ac* plane is almost 1 order of magnitude larger but its increase is much more dispersed in temperature. This is a strong indication of a

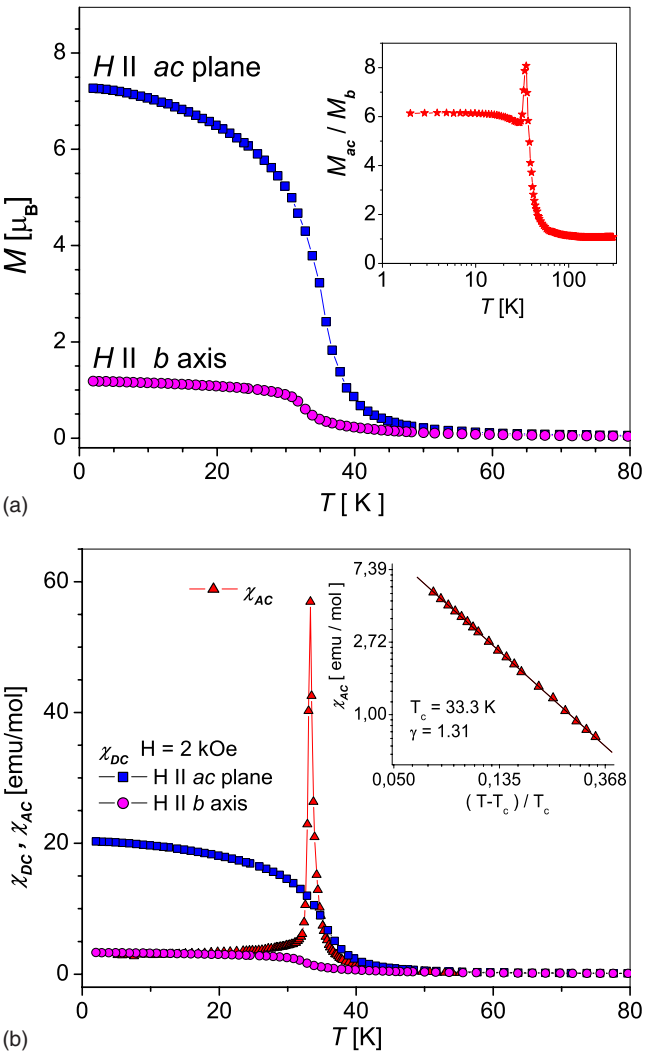

FIG. 3. (Color online) (a) Magnetization on cooling in field of 2 kOe set parallel and perpendicular to the *ac* plane. Inset: the ratio of the corresponding magnetizations. (b) The same data presented as dc susceptibility compared to ac susceptibility for powder sample. Inset: the log-log plot of the critical scaling of χ_{ac}.

different mechanism of ordering in the *ac* plane and perpendicular to that plane. It is clearly seen in the inset of Fig. 3(a) where the ratio of the two magnetizations M_{ac}/M_b is shown. This ratio is almost constant below the transition but when approaching the transition point displays a peak. The same data presented as dc susceptibility χ_{dc} are compared in Fig. 3(b) to the in-phase ac susceptibility χ_{ac} measured for the powder sample with the amplitude of the oscillating field equal to 2 Oe and the frequency of 125 Hz. One can notice that χ_{ac} drops suddenly just below T_c and levels off at a value close to χ_{dc} for H parallel to the *b* axis. χ_{ac} does not depend on frequency as checked in the range of 5–10 000 Hz for the powder sample.[18] The χ_{ac} critical exponent $\gamma=1.31\pm0.1$, determined from the classical fit in the temperature range of 35.7–44.5 K [see inset to Fig. 3(b)], is very close to that predicted for a spin system with the *XY* anisotropy.

Magnetization process is also different for the two orientations, as is shown in Fig. 4. The measurements were per-

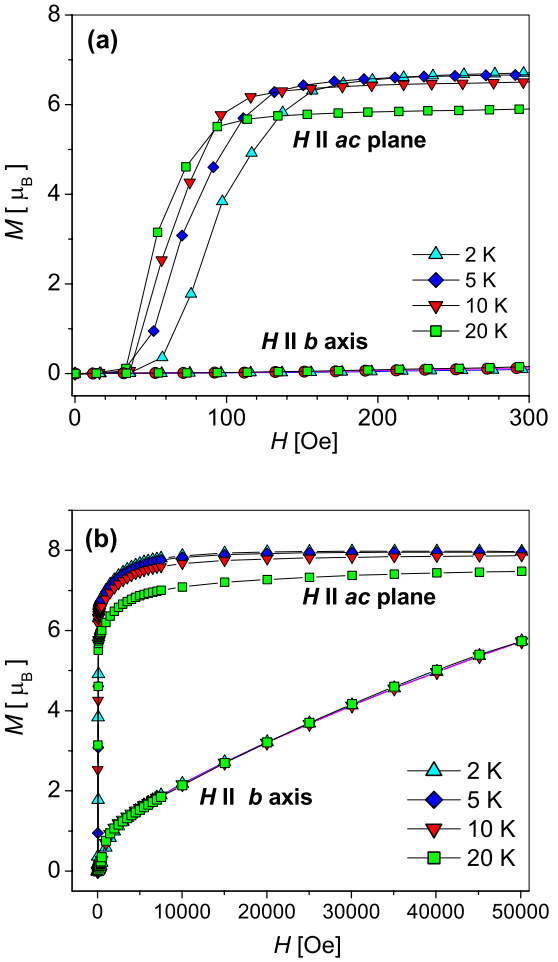

FIG. 4. (Color online) Magnetization as a function of applied magnetic field at different temperatures for the direction parallel to the *ac* crystallographic plane and that perpendicular to that plane. (a) Metamagnetic behavior is observed at small field values with the threshold value of about 50 Oe. (b) The *ac* plane is an easy plane and the *b* axis is a hard axis.

formed at three different temperatures: 2, 10, and 20 K. In the *ac* plane a metamagnetic behavior is observed; i.e., below the threshold field of about 50 Oe no magnetization is detected. Above that value the saturation is attained rather easily. The critical field H_{sf} for spin flip defined as the field of the largest dM/dH slope decreases with temperature and is equal to 84.5 Oe at 2 K, 60.5 Oe at 10 K, and 52 Oe at 20 K. By turning the crystal around the direction perpendicular to the petal face a weak anisotropy of magnetization within the *ac* plane was detected. On the other hand if the external field is applied perpendicular to the *ac* plane the magnetization process becomes almost temperature independent and even at 50 kOe it is far from reaching saturation. A similar feature is observed with hysteresis loops. Figure 5 shows the hysteresis loops obtained for the field lying in the *ac* plane. While magnetic field is increased from 0 to ≈50 Oe no magnetic moment is induced. Then a spin flip occurs and the loop opens up with saturation at the field of the order of 300 Oe. If one applies magnetic field perpendicular to the *ac* plane an unusual hysteresis loop is observed, cf. Fig. 6. The

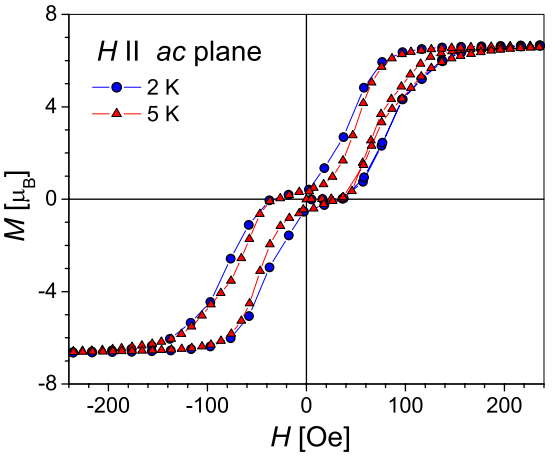

FIG. 5. (Color online) Hysteresis loop as obtained in the *ac* crystallographic plane at $T=2$ and 5 K.

normal loop opens only for $H \gg 300$ Oe as is shown in the inset of Fig. 6.

Temperature dependences of magnetization for ZFC and FC regimes with the field $H=20$ Oe set parallel to the *ac* plane or to the *b* axis is shown in Fig. 7. The FC magnetization drop at $T=T_c$ is noticeable. Keeping in mind the H_{sf} critical field which decreases with temperature [see Fig. 4(a)] one would expect a smoother $M(T)$ dependence below the transition temperature. Most probably the reason for such behavior is the relatively large time scale of the magnetization change. However, as may be seen from Fig. 8, the FC magnetization run at $H=50$ Oe is already more conventional.

B. Calorimetry

In order to further characterize the phase-transition calorimetric measurements have been performed. The heat-capacity measurement on a powder sample revealed an

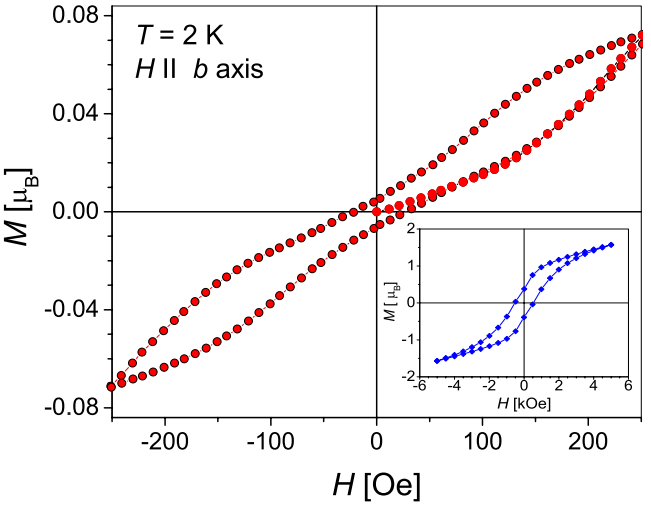

FIG. 6. (Color online) Hysteresis loop as obtained in the direction perpendicular to the *ac* plane at $T=2$ K. Inset: high-field sweep.

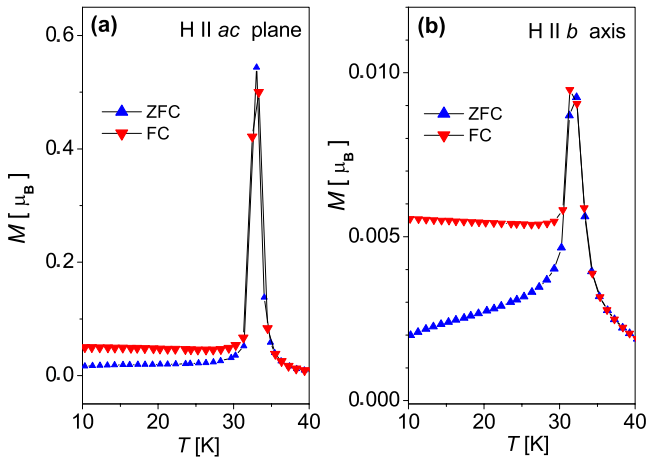

FIG. 7. (Color online) ZFC and FC magnetizations in the field $H=20$ Oe parallel to the (a) *ac* plane and (b) to the *b* axis.

anomaly around 34 K.[16] Here we include the heat-capacity data obtained for a single-crystal sample. The petal shape of the sample allowed to perform the measurement with magnetic field applied perpendicular to the *ac* plane. Such a positioning of the sample ensured, at the same time, a good thermal contact with the measuring unit. In Ref. 17 a simple model has been put forward to explain the changes in entropy and in the peak temperature with the external magnetic field. The details of data analysis were not presented. As these were far from trivial we give these below together with additional comments.

The task of primary importance was to extract the magnetic part from the overall heat capacity $C_p(T)$. The latter, for the nonconducting material, can be written as

$$C_p(T) = C_L(T) + C_M(T), \tag{1}$$

where C_L and C_M denote the lattice and magnetic contributions, respectively. In order to extract the magnetic contribution a specific approach was adopted.[22] The method consists of measuring C_p as a function of temperature at zero magnetic field and at high applied field. If the magnetic field is sufficiently large so that the magnetic system is in the spin-aligned paramagnetic state, the magnetic contribution to C_p will be suppressed and thus permitting one to find C_M as the difference between the zero- and high-field C_p at the temperature range of the heat-capacity anomaly. In Fig. 9 the zero-field and high-field C_p data are shown on a log-log plot in the temperature range $25<T<40$ K. The zero-field heat-capacity data, $C_p(T;0)$, show a relatively broad anomaly at about $T\simeq 33$ K, while the heat capacity $C_p(T;H^*)$, where $H^*=90$ kOe indicates a suppression of the zero-field anomaly together with the downshift of the zero-field values. Figure 10 shows magnetic-field dependence of the percentage downshift of the heat capacity defined by

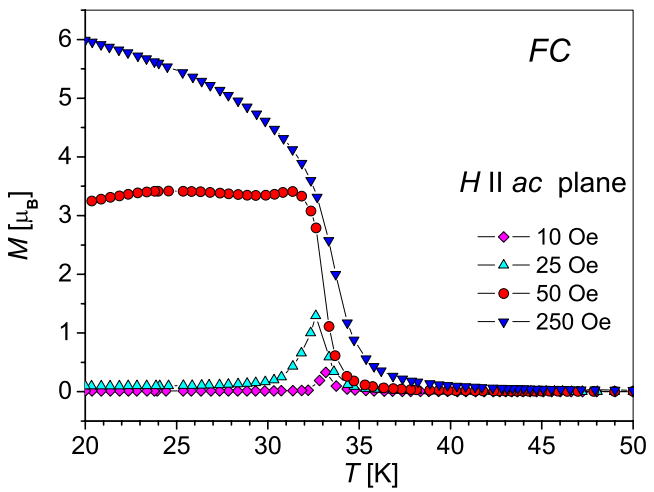

FIG. 8. (Color online) FC magnetization in the field parallel to *ac* plane for several H values.

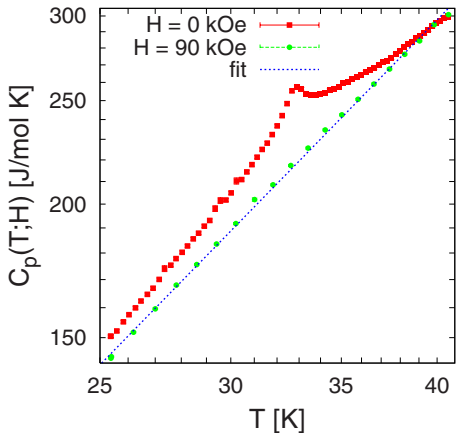

FIG. 9. (Color online) Zero-field and high-field heat capacities. The anomaly in the zero-field heat capacity (at $T\simeq 33$ K) is suppressed in the high-field data. The curve drawn through the high-field is a polynomial in T fitted to the data points and used in what follows to determine experimental $C_M(T;H)$ curves. For higher temperatures the high-field data surmount the zero-field data.

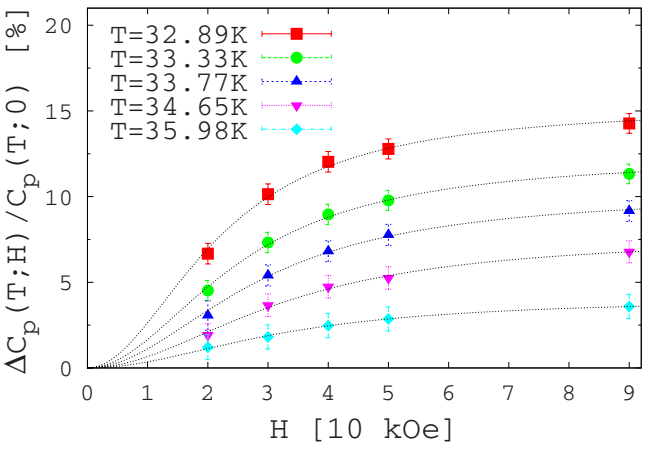

FIG. 10. (Color online) Magnetic field dependence of the percentage downshift of the heat capacity for several indicated temperatures. The data for $H=10$ kOe have been omitted because of large errors due to the fact that low magnetic fields brought about only slight changes in C_p [of the order of a small fraction of $C_p(T;0)$]. The dotted lines serve as guides to the eyes.

TABLE I. Comparison of the downshift in heat capacity $\Delta C_p(T;H^*)/C_p(T;0)$ with the saturation values $\Delta C_p(T;H\to\infty)/C_p(T;0)$ obtained from the inverse slope (A/B) of plots shown in Fig. 12.

T (K)	A/B (%)	$\Delta C_p(T;H^*)/C_p(T;0)$ (%)
32.89	15.6	14.3
33.33	12.6	11.3
33.77	10.6	9.2
34.65	7.5	6.8
35.98	4.0	3.6

$$\frac{\Delta C_p(T;H)}{C_p(T;0)} = \frac{C_p(T;0) - C_p(T;H)}{C_p(T;0)} \tag{2}$$

for several indicated temperatures. It reveals that ΔC_p at a given temperature nearly saturates at the highest field; thus supporting our assumption that the spin-aligned paramagnetic state is well established at $H^*=90$ kOe. Referring to Fig. 10 and using Eq. (1), we can hence write

$$C_L(T) = C_p(T;H^*), \tag{3}$$

$$C_M(T;H) = C_p(T;H) - C_p(T;H^*). \tag{4}$$

In order to estimate errors in $C_L(T)$ and $C_M(T;H)$ in Eqs. (3) and (4) due to the incompleteness of the saturation of the curves shown in Fig. 10, we use the extrapolation scheme. If we describe the field dependence of the shift in C_p by the empirical relation,

$$\frac{\Delta C_p(T;H)}{C_p(T;0)} = \frac{AH^2}{1+BH^2}, \tag{5}$$

then it can be demonstrated that plots of $H^2/[\Delta C_p(T;H)/C_p(T;0)]$ vs H^2 are linear. The inverse of the slope (A/B) is equal to the limiting high-field value for the percentage downshift of C_p. In Table I we list the values of $\Delta C_p(T;H^*)/C_p(T;0)$ along with those of $\Delta C_p(T;H\to\infty)/C_p(T;0)$ obtained within the extrapolation scheme. The results indicate that $C_L(T)$ as determined by Eq. (3) is overestimated, whereas the $C_M(T;H)$ determined by Eq. (4) is underestimated by about 1% of the $C_p(T;0)$ values. It can further be seen that the uncertainty expressed relative to the $C_p(T;0)$ values diminishes with increasing temperature. With C_p steadily increasing, this means that the absolute error does not change considerably within the temperature window studied.

In Fig. 11 the magnetic heat capacities C_M determined using Eq. (4) are plotted for five indicated values of the external magnetic field. The C_M curves all show relatively broad peaks gradually suppressed by the increasing magnetic field. As the magnitude of the external magnetic field is increased, the shape of the peaks changes from a cusplike one to a broad bump covering the entire temperature range. It can be seen that the transition temperature shifts toward lower temperatures as the external magnetic field increases.

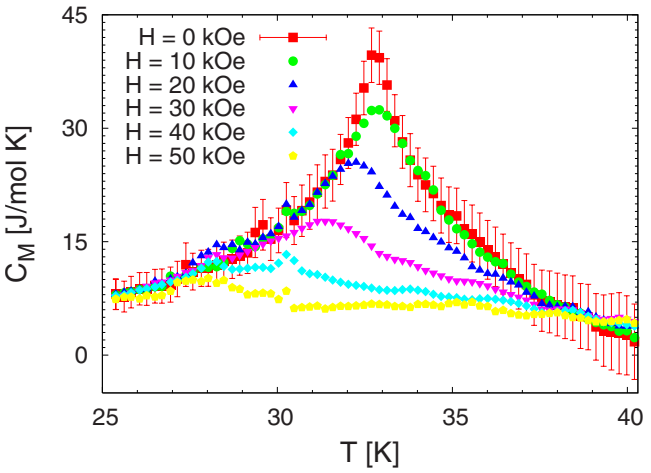

FIG. 11. (Color online) Magnetic heat capacity $C_M(T;H)$ determined by using Eq. (4) and the data shown in Fig. 9. For clarity only the error bars on the $C_M(T;0)$ curve have been shown. The main contribution to the errors comes from the incompleteness of the saturation of the curves depicted in Fig. 10. It results in the uncertainty of about 1% of the $C_p(T;0)$ values (see text).

The entropy associated with the phase transition is determined by integrating the experimental $C_M(T)$ data with respect to $\ln T$. The maximum expected value $S_{\max}$ is that for an array of eight one-half spins and thus equal to $R\ln(2J+1)$[8], where R is the gas constant and $J=1/2$, which yields $S_{\max}=46.1$ J/K mol. The entropy obtained in the zero external field amounts to 6.9 J/K mol, that is only 15% of the maximal expected value in agreement with the powder sample results. The low value of the entropy involved in the phase transition points to the presence of short-range correlations above the transition temperature. An increase in the correlation length on cooling leads to the development of a state of ordered clusters.

It is a well-known fact that the presence of a strong easy-plane anisotropy is a prerequisite to the transition of the Berezinskii-Kosterlitz-Thouless type in 2D systems.[9–11] Monte Carlo simulations for 2D *XXZ* model on a square lattice,[23] which is closest to our bilayered system, show that for all values of the easy-plane anisotropy parameter there is a signature of the BKT transition. The qualitative behavior of the heat capacity was observed to be the same with a maximum displayed at a temperature of about 10% above the transition temperature. The maxima obtained had a cusplike shape and became broader and much less pronounced while approaching the isotropic limit. Although the shape of the heat-capacity anomaly obtained by us at zero field is consistent with the numerical results (see Fig. 11), our magnetic and thermal data do not exhibit a separation between the transition temperature and the heat-capacity peak temperature. That may be due to the fact that the spins are located at the sites of a double-layer lattice instead of a single 2D one.

IV. DISCUSSION

The important issue in the study of layered compounds is to understand magnetic interactions in a molecular network.

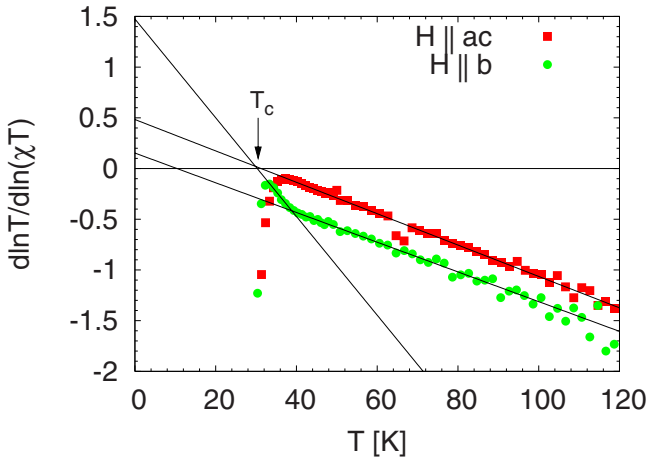

FIG. 12. (Color online) Critical scaling analysis. The $d \ln T/d \ln(\chi T)$ vs T plots for the direction parallel to the *ac* plane and that perpendicular to that plane.

In the present case we have to distinguish between the interactions within the bilayer and those between the bilayers. According to the crystallographic data W-CN-Cu bridges along the *b*-crystallographic axis are almost linear. As a result the magnetic orbitals of the W and Cu ions are orthogonal and the interaction is ferromagnetic. In the *ac* plane the issue is less clear as the cyanobridges are slightly bent. As mentioned earlier the interaction between the bilayers is expected to be of an antiferromagnetic character. In view of the fact that there are no obvious candidates for the interaction pathways, the conjecture arises that the interbilayer coupling is of dipolar origin, as it is in the case of hydroxides reported by Panissod and Drillon.[24]

A. Static scaling analysis

To gain a more precise insight into the character of the ordering process we performed an analysis of the static critical scaling of the magnetic susceptibility in the form outlined and applied in a series of illuminating papers.[25–28] The magnetization data collected in the field of 2 kOe (cf. Fig. 3) were appropriately rescaled to yield the dc magnetic susceptibility. For both orientations of the sample the fits to the Curie-Weiss law; i.e., $\chi = C/(T-\theta)$ were performed. The best-fit results gave $C_{\|}=3.86$ emu K/mol and $\theta_{\|}=53.7$ K for the susceptibility in the direction parallel to the *ac* plane and $C_{\perp}=3.79$ emu K/mol and $\theta_{\perp}=51.0$ K in the direction perpendicular to that plane. The values and signs obtained for the Weiss constants indicate the presence of the ferromagnetic coupling of the order of tens of Kelvin in the spin network. Figure 12 shows the plot of the $d \ln T/d \ln(\chi T)$ against temperature. One can see that the data tend to align in the pretransitional high-temperature region. The linear fits revealed the values of the corresponding transition temperatures T_c (the intersection with the abscissa axis) and the critical exponents (the inverses of the intersection point with the ordinate axis). The corresponding errors were estimated to account for the dependence on the temperature range and the measurement uncertainties. In the direction parallel to the *ac* crystallographic plane the system can be said to undergo a direct transition at $T_{c\|}=31.2\pm2.3$ K displaying a rather high value of $\gamma_{\|}=2.0\pm0.3$. The behavior in the direction perpendicular to the bilayers plane is more striking, revealing a crossover at temperature $\approx$38.8 K from a region with an exceptionally high value of the gamma exponent 6.8 ± 1.8 and the presumed transition temperature at 10.4 ± 1.5 K to the state characterized by a low value of $\gamma_{\perp}=0.67\pm0.04$ and the transition temperature of $T_{c\perp}=30.3\pm3.4$ K. The T_c's for both the directions have close values which points to the fact that the transition in the *ac* plane triggers that in the direction perpendicular to the *ac* plane. The unusually high value of γ in the precrossover region is consistent with a relatively rapid increase in the magnetization in the direction perpendicular to the *ac* plane observed on lowering the temperature, cf. Fig. 3(a), and suggests the scaling behavior close to the exponential one. The exponential regime as is well known[29] is a characteristic of 2D systems, for which the transition is said to occur only at $T_c=0$ K.[8,30]

By contrast, the transition for the directions parallel to the bilayers is a one-stage process. Its most intriguing feature is a rather high value of the γ exponent which fails to agree with any values known for the three-dimensional ferromagnetic ordering processes ($\gamma\sim1.24$ for Ising, 1.32 for *XY*, and 1.385 for Heisenberg spins). On the other hand, it is consistent with the values obtained in the numerical simulations of the 2D classical *XY* model[31] ($\gamma=1.82$) or more pertinent to the case of the 2D classical *XXZ* model ($\gamma=2.17\pm0.05$ for $\lambda=0.99$) under study.[23] That speaks in favor of the transition being of the Berezinskii-Kosterlitz-Thouless type[9–11] where the magnetic susceptibility is predicted to obey the following critical behavior:

$$\chi T = a_{\chi} e^{b_{\chi}(T-T_{\mathrm{BKT}})^{-\nu}}, \tag{6}$$

with the exponent $\nu=0.5$. To verify that conjecture we proceeded to perform a corresponding fit. We performed a nonlinear fit in the transformed coordinates of $\{T, -dT/d\ln(\chi T)\}$ to the function $f(T) = 1/(b_{\chi}\nu)(T-T_{\mathrm{BKT}})^{\nu+1}$ which yielded $T_{\mathrm{BKT}}=30.3\pm2.7$ K, $\nu=0.56\pm0.11$, and $b_{\chi}=12.8\pm4.2$ [note its dimension being $(\mathrm{K})^{\nu}$]. Then the result was depicted in the linearized form provided in Fig. 13. As can be seen the points align in a quite wide temperature range reaching up to $\sim$120 K. Such a wide critical region $\Delta T\sim 2T_c$ is very similar to that reported for the spin-1/2 2D Heisenberg model.[32] The value of ν is consistent within the error with that predicted by Kosterlitz and Thouless.[10] From the temperature of the BKT transition obtained in the scaling analysis one may try to get information on the magnetic coupling constant. The occurrence of the BKT transition in the ferromagnetic case with the exchange anisotropy is born out by numerical simulations.[23,33,34] It has been shown that in the isotropic limit the transition disappears logarithmically,[35,36] i.e., $T_{\mathrm{BKT}}\sim[-\ln(1-\lambda)]^{-1}$, where $\lambda=J_{zz}/J_{xx(yy)}$ is the exchange anisotropy parameter. It can be even estimated that λ must be lower than about 0.78, the value which was shown to be the critical degree of exchange anisotropy above which the BKT transition is destroyed due to quantum isotropization for a spin-1 *XXZ* model.[37] As our system is that of two ferromagnetically coupled layers we can expect its behavior to go

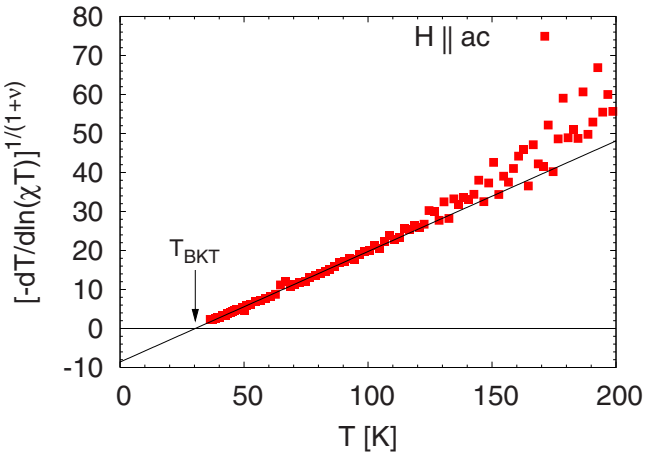

FIG. 13. (Color online) The Berezinskii-Kosterlitz-Thouless transition hallmark. The $[-dT/d\ln(\chi T)]^{1/(\nu+1)}$ vs T plot of the data for the direction parallel to the *ac* plane.

somewhere between a 2D network of spins 1/2 and that of spins 1. The transition temperatures for those systems were found to amount to $t_c = T_{BKT}/J \sim 0.36$ and 0.49, respectively, which stays in very good agreement with the quantum Monte Carlo simulations.[34] Hence, and using the transition temperature value obtained in the fit, we can estimate the value for the equatorial in-plane exchange constant $J_{xx(yy)} \in (61.8, 84.2)$ K. Another way of estimating that exchange coupling constant is by means of the parameter b_χ which may be compared with the results obtained in the Monte Carlo simulations. Assuming $\nu = 0.5$ the numerical simulation of the classical *XXZ* model[23] for $\lambda = 0.5$ implies that $J_{xx(yy)} \in (30, 63.7)$ K where the lower value was assumed not to fall below T_{BKT}. It is consistent with the upper bound determined above but may still be underestimated; as for the quantum model one expects b_χ to diminish. The exchange coupling between the spins belonging to either of the layers in the bilayer is implied to be also ferromagnetic and exceeds 80 K as exhibiting an almost linear geometry of the mediating cyanobridge.

There is one more way to estimate the average intralayer exchange interaction in our system. For a 2D system with a weak interlayer interaction J' and the intralayer coupling J, it is predicted that[38]

$$k_B T_c/J = \frac{4}{\ln(J/J')}, \tag{7}$$

where k_B is the Boltzmann constant. The order of the antiferromagnetic coupling J' between the bilayers can be estimated from the saturation field H_{AF} in the easy-plane direction. Inserting $H_{AF} \approx 100$ Oe [see Fig. 4(a)] into the equation $g\mu_B H_{AF} = 2z|J'|S$ one arrives at $J' = 7.5$ mK. Taking $T_c \approx 33$ K and using Eq. (7) one obtains the average intrabilayer exchange integral $J = 77.5$ K, the value which compares well with the previous estimates. Moreover, it is consistent with the quantum Monte Carlo predictions.[39] On the basis on the values of two ratios, $T_c/J = 0.43$ and $J/J' \approx 10^4$, we can state that the WCuT molecular magnet may be regarded as an almost 2D magnet. In comparison to some other copper-based quasi-2D magnets[40] it has a rather high T_c/J value due to its bilayered structure.

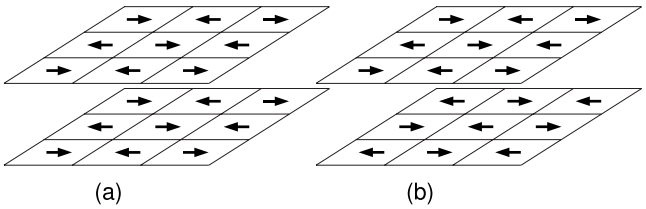

FIG. 14. Configurations corresponding to (a) ferromagnetic and (b) antiferromagnetic orderings of clusters belonging to adjacent bilayers assuming an easy-plane anisotropy.

B. Dipolar interactions and metamagnetic behavior

The metamagnetic behavior displayed by the system in the direction parallel to the *ac* plane, cf. Fig. 4(a), is yet another key feature revealed by the magnetic single-crystal studies. As can be seen at fields lower than a threshold value of about 100 Oe very small or no magnetic moment is induced. The value of the spin-flip field indicates that the interaction responsible for suppression of the magnetization must be rather weak. We believe that it originates from the dipolar spin-spin interactions acting effectively as antiferromagnetic due to the in-plane confinement of the spins below the transition. Such an effect has been observed in a similar double-layer compound based on octacyanometallates.[41] Assuming the presence of clusters of correlated spins within the bilayers as depicted in Fig. 14 and the magnetic dipole-dipole interactions, the energy difference between the ferromagnetic and antiferromagnetic ordering of clusters was calculated. For the in-plane orientation of the spins the antiferromagnetic configuration has lower energy. Such a picture of uniformly ordered clusters is plausible at lower temperatures where the gas of vortex-antivortex pairs is expected to be diluted.[42] The result was expressed in terms of the magnetic field acting on the spin of a single ion (spin 1/2). The discrete distribution of magnetic moments was approximated by a uniform continuous magnetic-moment density smeared over the double-layer plane. The contributions from double layers contained in a cube of linear dimension $(2K+1)(2N+1)$ unit-cell spacings were summed up, where $(2K+1)(2K+1)$ is the number of clusters in the double-layer plane, and $(2N+1)(2N+1)$ is the number of unit cells per a single cluster. The orientation of the magnetic moments of clusters was parametrized by a couple of spherical angles (θ, ϕ) defined with respect to the x, y, z axes coinciding with the c, a, and b crystallographic axes, respectively. Such a problem can be integrated out completely so that the numerical procedure simplifies greatly. The numerical calculation saturates very quickly with K so that even for $K=0$ and 1 it yields very close values. It is therefore reasonable to quote the formula corresponding to the simplest case of one cluster per a double layer ($K=0$). It reads

$$H(\theta, \phi) = (\sin^2\theta \sin^2\phi - \cos^2\theta)H_a - (\sin^2\theta \cos^2\phi - \cos^2\theta)H_c, \tag{8}$$

where H_a and H_c correspond to the orientation of the mag-

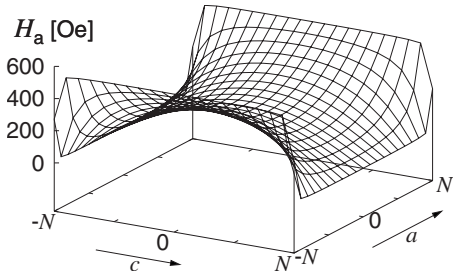

FIG. 15. Distribution of the field H_a calculated assuming $g=2$, $S=1/2$, $n=4$, $\theta=\pi/2$, $K=5$, and $N=500$. The shape of the distribution in the case of the moments oriented along the c axis (H_c) is obtained by its in-plane rotation through $\pi/2$.

netic moments along the a and c crystallographic axes, respectively, and are given by the formulas,

$$H_a = \frac{4\mu_0\mu_B ngS}{\pi abc}\arctan\left[\frac{bc}{a\sqrt{a^2+b^2+c^2}}\right], \tag{9}$$

$$H_c = \frac{4\mu_0\mu_B ngS}{\pi abc}\arctan\left[\frac{ab}{c\sqrt{a^2+b^2+c^2}}\right], \tag{10}$$

where μ_B is the Bohr magneton, g is the gyromagnetic factor, S is the spin number of a single ion, and n is the number of ions per crystallographic cell contained in one double layer. Figure 15 shows the distribution of the field H_a calculated assuming $g=2$, $S=1/2$, $n=4$, $\theta=\pi/2$, $K=5$, and $N=500$. The continuous approximation used by us implies that the size of the cluster should be larger than the interlayer distance, hence the choice for N. The values averaged over the entire cluster $\bar{H}_a$ and $\bar{H}_c$ have been found to amount to 270 and 290 Oe, respectively. They are higher than the value of the critical field revealed in the measurement but this is partially due to the fact that in the calculation a very regular pattern of clustering was considered as depicted in Fig. 14. In reality the clusters may differ in size and their positions are randomly distributed over the double layers. Another reason is the assumption that the magnetic moments of the clusters are strictly confined to the double layers plane. Equation (8) indicates that for the configuration with moments standing out of that plane the value of the spin-flip field will be lowered. Demanding, e.g., that $H_c(\theta)\equiv H(\theta,0)=H_0$ one readily obtains $\theta_c=\arctan\sqrt{(H_0+\bar{H}_a+\bar{H}_c)/(\bar{H}_c-H_0)}$. For $H_0\approx 100$ Oe one gets $\theta_c\approx 76°$, which means we reproduce the experimental values if the magnetic moments form an angle of about 15° with the plane of the double layer.

V. CONCLUSIONS

The pattern of magnetic interactions revealed by single-crystal studies of our bilayered molecular magnet can thus be concluded as follows: the rather strong average in-plane exchange coupling of about 80 K together with the easy-plane exchange anisotropy drive the system to undergo the BKT transition at about 31 K. The weak coupling between the bilayers, presumably of the dipolar origin, is responsible for the stabilization of the 3D overall antiferromagnetic order. The small value of $\gamma_\perp \sim 0.7$ observed in the direction perpendicular to the ac plane implies that the correlations in the vertical direction is a mere by-product of the BKT transition. The spontaneous creation of vortices and the ensuing creation of vortex-antivortex pairs more and more tightly bound, while approaching the T_{BKT} temperature from above leads to the more and more pronounced correlations of the out-of-plane spin components, which is signaled by the abrupt increase in the field-cooled magnetization [cf. Fig. 3(a)]. The heat-capacity measurements revealed a reduced value of entropy change associated with the transition pointing to a well-established state of short-range order above the transition. This feature is consistent with the wide temperature range of critical scaling indicating a 2D character of local ordering above the transition temperature.

ACKNOWLEDGMENTS

This work was partially financed by Polish Committee for Scientific Research (KBN) under Grant No. 0087-B-H03-2008-34. One of the authors (T.W.) expresses his gratitude to the staff of the Research Center for Molecular Thermodynamics at Osaka University for their kind hospitality and instructive discussions.

*robert.pelka@ifj.edu.pl

[1] J.-C. G. Bunzli and C. Piguet, Chem. Rev. (Washington, D.C.) **102**, 1897 (2002).
[2] B. Sieklucka, R. Podgajny, P. Przychodzeń, and T. Korzeniak, Coord. Chem. Rev. **249**, 2203 (2005).
[3] Y. Song, S. Ohkoshi, Y. Arimoto, H. Seino, Y. Mizobe, and K. Hashimoto, Inorg. Chem. **42**, 1848 (2003).
[4] H. Z. Kou, Z. H. Ni, B. C. Zhou, and R. J. Wang, Inorg. Chem. Commun. **7**, 1150 (2004).
[5] R. Podgajny, T. Korzeniak, K. Stadnicka, Y. Dromzee, N. W. Alcock, W. Errington, K. Kruczała, M. Bałanda, T. J. Kemp, M. Verdaguer, and B. Sieklucka, Dalton Trans. **2003**, 3458.
[6] Z. J. Zhong, H. Seino, Y. Mizobe, M. Hidai, A. Fujishima, S. Ohkoshi, and K. Hashimoto, J. Am. Chem. Soc. **122**, 2952 (2000).
[7] E. Coronado, J. Galan-Mascaros, C. Gomez-Garcia, and V. Laukhin, Nature (London) **408**, 447 (2000).
[8] N. D. Mermin and H. Wagner, Phys. Rev. Lett. **17**, 1133 (1966).
[9] V. L. Berezinskii, Zh. Eksp. Teor. Fiz. **59**, 907 (1970).
[10] J. M. Kosterlitz and D. J. Thouless, J. Phys. C **6**, 1181 (1973).
[11] J. M. Kosterlitz, J. Phys. C **7**, 1046 (1974).
[12] S. T. Bramwell and P. C. W. Holdsworth, J. Phys.: Condens. Matter **5**, L53 (1993).
[13] S. T. Bramwell and P. C. W. Holdsworth, J. Appl. Phys. **73**, 6096 (1993).
[14] A. Taroni, S. T. Bramwell, and P. C. W. Holdsworth, J. Phys.:

Condens. Matter **20**, 275233 (2008).
[15] P. Przychodzeń, T. Korzeniak, R. Podgajny, and B. Sieklucka, Coord. Chem. Rev. **250**, 2234 (2006).
[16] R. Podgajny, T. Korzeniak, M. Bałanda, T. Wasiutyński, W. Errington, T. J. Kemp, N. W. Alcock, and B. Sieklucka, Chem. Commun. (Cambridge) **2002**, 1138.
[17] R. Pełka, M. Bałanda, T. Wasiutyński, Y. Nakazawa, M. Sorai, R. Podgajny, and B. Sieklucka, Czech. J. Phys. **54**, 595 (2004).
[18] M. Bałanda, T. Korzeniak, R. Pełka, R. Podgajny, M. Rams, B. Sieklucka, and T. Wasiutyński, Solid State Sci. **7**, 1113 (2005).
[19] F. L. Pratt, P. M. Zieliński, M. Bałanda, R. Podgajny, T. Wasiutyński, and B. Sieklucka, J. Phys.: Condens. Matter **19**, 456208 (2007).
[20] U. Bovensiepen, C. Rudt, P. Poulopoulos, and K. Baberschke, J. Magn. Magn. Mater. **231**, 65 (2001).
[21] C. Rudt, P. Poulopoulos, J. Lindner, A. Scherz, H. Wende, K. Baberschke, P. Blomquist, and R. Wappling, Phys. Rev. B **65**, 220404(R) (2002).
[22] M. Shayegan, M. S. Dresselhaus, L. Salamanca-Riba, G. Dresselhaus, J. Heremans, and J.-P. Issi, Phys. Rev. B **28**, 4799 (1983).
[23] A. Cuccoli, V. Tognetti, and R. Vaia, Phys. Rev. B **52**, 10221 (1995).
[24] P. Panissod and M. Drillon, in *Magnetism: Molecules to Materials IV*, edited by J. S. Miller and M. Drillon (Wiley, New York, 2003), p. 223.
[25] M. Fahnle and J. Souletie, J. Phys. C **17**, L469 (1984).
[26] E. Carré and J. Souletie, J. Magn. Magn. Mater. **72**, 29 (1988).
[27] C. Paulsen, J. Souletie, and P. Ray, J. Magn. Magn. Mater. **226-230**, 1964 (2001).
[28] M. Drillon, P. Panissod, P. Rabu, J. Souletie, V. Ksenofontov, and P. Gutlich, Phys. Rev. B **65**, 104404 (2002).
[29] F. Suzuki, N. Shibata, and C. Ishii, J. Phys. Soc. Jpn. **63**, 1539 (1994).
[30] N. D. Mermin, Phys. Rev. **176**, 250 (1968).
[31] R. Gupta, J. DeLapp, G. G. Batrouni, G. C. Fox, C. F. Baillie, and J. Apostolakis, Phys. Rev. Lett. **61**, 1996 (1988).
[32] H.-Q. Ding and M. S. Makivić, Mod. Phys. Lett. B **4**, 697 (1990).
[33] A. Cuccoli, V. Tognetti, P. Verrucchi, and R. Vala, J. Appl. Phys. **76**, 6362 (1994).
[34] H.-Q. Ding and M. S. Makivić, Phys. Rev. B **42**, 6827 (1990).
[35] S. B. Khokhlachev, Zh. Eksp. Teor. Fiz. **70**, 265 (1976).
[36] S. Hikami and T. Tsuneto, Prog. Theor. Phys. **63**, 387 (1980).
[37] A. Cuccoli, V. Tognetti, P. Verrucchi, and R. Vaia, J. Magn. Magn. Mater. **140-144**, 1703 (1995).
[38] V. Pokrovsky and G. Uimin, in *Magnetic Properties of Layered Transition Metal Compounds*, edited by L. de Jongh (Kluwer, Dordrecht, 1990), p. 53.
[39] C. Yasuda, S. Todo, K. Hukushima, F. Alet, M. Keller, M. Troyer, and H. Takayama, Phys. Rev. Lett. **94**, 217201 (2005).
[40] S. Blundell, T. Lancaster, F. Pratt, P. Baker, M. Brooks, C. Baines, J. Manson, and C. Landee, J. Phys. Chem. Solids **68**, 2039 (2007).
[41] S. Kaneko, Y. Tsunobuchi, S. Sakurai, and S. Ohkoshi, Chem. Phys. Lett. **446**, 292 (2007).
[42] J. Tobochnik and G. V. Chester, Phys. Rev. B **20**, 3761 (1979).